Microbiology (2009), **155**, 3121–3133 DOI 10.1099/mic.0.029157-0

Lectin mapping reveals stage-specific display of surface carbohydrates in *in vitro* and haemolymph-derived cells of the entomopathogenic fungus *Beauveria bassiana*

Arun Wanchoo, Michael W. Lewis and Nemat O. Keyhani

Department of Microbiology and Cell Science, University of Florida, Gainesville, FL 32611, USA

Correspondence
Nemat O. Keyhani
keyhani@ufl.edu

Received 13 March 2009
Revised 29 June 2009
Accepted 9 July 2009

The entomopathogenic fungus *Beauveria bassiana* and its insect host target represent a model system with which to examine host–pathogen interactions. Carbohydrate epitopes on the surfaces of fungal cells play diverse roles in processes that include adhesion, non-self recognition and immune invasion with respect to invertebrate hosts. *B. bassiana* produces a number of distinct cell types that include aerial conidia, submerged conidia, blastospores and haemolymph-derived cells termed *in vivo* blastospores or hyphal bodies. In order to characterize variations in the surface carbohydrate epitopes among these cells, a series of fluorescently labelled lectins, combined with confocal microscopy and flow cytometry to quantify the response, was used. Aerial conidia displayed the most diverse lectin binding characteristics, showing reactivity against concanavalin A (ConA), *Galanthus nivalis* (GNL), *Griffonia simplicifolia* (GSII), *Helix pomatia* (HPA), *Griffonia simplicifolia* isolectin (GSI), peanut agglutinin (PNA), *Ulex europaeus* agglutinin I (UEAI) and wheatgerm agglutinin (WGA), and weak reactivity against *Ricinus communis* I (RCA), *Sambucus nigra* (SNA), *Limax flavus* (LFA) and *Sophora japonica* (SJA) lectins. Lectin binding to submerged conidia was similar to that to aerial conidia, except that no reactivity against UEAI, HPA and SJA was noted, and WGA appeared to bind strongly at specific polar spots. In contrast, the majority of *in vitro* blastospores were not bound by ConA, GNL, GSII, GSI, SNA, UEAI, LFA or SJA, with PNA binding in large patches, and some polarity in WGA binding noted. Significant changes in lectin binding also occurred after aerial conidial germination and in cells grown on either lactose or trehalose. For germinated conidia, differential lectin binding was noted between the conidial base, the germ tube and the hyphal tip. Fungal cells isolated from the haemolymph of the infected insect hosts *Manduca sexta* and *Heliothis virescens* appeared to shed most carbohydrate epitopes, displaying binding only to the GNL, PNA and WGA lectins. Ultrastructural examination of the haemolymph-derived cells revealed the presence of a highly ordered outermost brush-like structure not present on any of the *in vitro* cells. Haemolymph-derived hyphal bodies placed into rich broth medium showed expression of several surface carbohydrate epitopes, most notably showing increased PNA binding and strong binding by the RCA lectin. These data indicate robust and diverse production of carbohydrate epitopes on different developmental stages of fungal cells and provide evidence that surface carbohydrates are elaborated in infection-specific patterns.

INTRODUCTION

The ascomycete *Beauveria* (*Cordyceps*) *bassiana* displays a unique lifestyle, as it is a broad-host-range entomopathogenic fungus that is also a saprophyte found in soil, and can form endophytic relationships with various plants. Infection of insects begins with attachment of conidia to hosts, followed by germination and elongation of conidial germ tubes that penetrate the cuticle. The growing hyphae reach the haemocoel, where they elaborate yeast-like cells termed *in vivo* blastospores or hyphal bodies that evade the insect immune system and proliferate in the haemolymph. Ultimately, the hyphal bodies form elongating hyphae which emerge from the insect cadaver, producing conidiophores for dispersal. Throughout this process, the interaction between the pathogen and the host is mediated by the fungal cell wall, which is able to respond to diverse

Abbreviations: DIC, differential interference contrast; PI, propidium iodide; TEM, transmission electron microscopy.

surface cues and nutrient availability (Holder & Keyhani, 2005; Holder *et al.*, 2007; Lewis *et al.*, 2009). Little is known concerning the arrangement of carbohydrate molecules on the surfaces of the different developmental stages of the fungus, although such changes may have important consequences regarding adhesion, host detection, cuticle penetration and non-self recognition by host defence mechanisms. Lectins represent relatively simple probes for the identification of specific carbohydrate residues on the surfaces of cells, and have been extensively used to characterize fungal cell walls, including particularly the examination of host–pathogen interactions (Lis & Sharon, 1986; Sharon & Lis, 1993; Sharon, 2007). Differences in surface constituents during fungal growth and among various developmental stages may influence host–parasite interactions, and alternations in surface mannose, glucose and sialic acid epitopes in *Candida albicans* and *Aspergillus fumigatus* have been linked to their ability to infect and colonize hosts as well as to activate immune cells and cytokine production (Esquenazi *et al.*, 2003; Latgé *et al.*, 1994; Masuoka, 2004; Warwas *et al.*, 2007).

Several studies have highlighted the importance of fungal surface carbohydrates in mediating fungal–insect pathogenesis. Shedding or changes in the galactomannan coat of the insect pathogenic fungus *Paecilomyces farinosus*, as determined by binding of galactose- and mannose-specific lectins to fungal cell wall surfaces, is thought to prevent opsonization of the fungal cell by the host, which attempts to coat invading particles with humoral factors such as lectins (Pendland & Boucias, 1993, 1996). Similarly, investigations of the carbohydrate constituents of the cell walls of the entomogenous hyphomycete *Nomuraea rileyi* have revealed the absence of galactose from haemolymph-derived hyphal bodies, a feature considered to be important for successful immune evasion, since galactose-specific lectins which would promote opsonization are common in insects (Pendland & Boucias, 1984, 1992). FITC-conjugated lectins have been used to investigate the cell surfaces of a number of entomopathogenic fungi, including *P. farinosus*, *N. rileyi*, *Metarhizium anisopliae* and *B. bassiana* (Pendland & Boucias, 1986). All the fungi tested were bound by concanavalin A (ConA) and wheatgerm agglutinin (WGA), whereas mycelia/blastospore mixtures of *P. farinosus* and *B. bassiana* were also bound by peanut agglutinin (PNA) and weakly by winged pea and soybean agglutinins (Pendland & Boucias, 1986). These studies, however, did not examine *B. bassiana* haemolymph-derived cells or the different cell types produced by the fungi. Using a series of fluorescently labelled lectins, we have performed a systematic characterization of the surface carbohydrate epitopes of various developmental stages of *B. bassiana*, including haemolymph-derived *in vivo* hyphal bodies and cells grown on lactose or trehalose, the latter substrate being the major carbohydrate constituent of the insect haemolymph. Our data indicate dynamic and robust changes in surface carbohydrate epitopes between the different cell types, including infection-specific hyphal bodies, as well as during growth of germinated conidia. Differential binding of specific lectins was also noted between the conidial base, the germ tube and the growing tip of germinated conidia, indicating that carbohydrate epitopes are dynamically altered during growth. The use of the fluorescently labelled lectins also allowed for the visualization of polarized spots and patches of carbohydrates on specific cells, and lectin binding was assessed quantitatively by flow cytometry.

METHODS

Fungal material. *B. bassiana* (ATCC 90517) was routinely grown on Potato dextrose agar (PDA). Plates were incubated at 26 °C for 10–14 days and aerial conidia were harvested by flooding the plate with sterile distilled H_2O. Conidial suspensions were filtered through a single layer of Miracloth and final spore concentrations were determined by direct counting using a haemocytometer. Blastospores were produced in Sabouraud dextrose + 0.5 % yeast extract (SDY) liquid broth cultures using conidia harvested from plates to a final concentration of $0.5–5 \times 10^5$ conidia ml^{-1} as the inoculum. Cultures were grown for 3–4 days at 26 °C with aeration. Cultures were filtered (twice) through glass wool to remove mycelia, and the concentration of blastospores was determined by direct counting. Submerged conidia were produced in TKI broth using fructose as the carbon source, as described by Thomas *et al.* (1987). For all (*in vitro*) single-cell types, Miracloth- or glass wool-filtered cell suspensions were harvested by centrifugation (7000 ***g***, 5 min, 4 °C), washed once with medium, and resuspended to the desired concentration (typically $10^7–10^8$ cells ml^{-1}). Hyphae were produced by inoculation of SDY media by aerial conidia. Cultures were allowed to grow for 12–24 h at 26 °C and the resultant cell suspension was harvested by centrifugation and washed as described above. The production of *in vivo* fungal cells was performed essentially as described by Tartar & Boucias (2004). Two different insect systems were used to isolate *B. bassiana*-derived *in vivo* cells. Briefly, the tobacco budworm *Heliothis virescens* and *Manduca sexta* were used as hosts to isolate *in vivo* fungal cells. Third to fifth larval instars reared on an artificial diet at 25 °C were challenged by injection of either (*in vitro*) blastospores or aerial conidia ($2–5 \times 10^4$ cells per larva) into the haemocoel. Injected larvae were incubated for 68–72 h at 25 °C, after which individual larvae were injected with 0.5 ml anticoagulant solution (0.14 M NaCl, 0.1 M glucose, 26 mM citric acid, 30 mM trisodium citrate, 10 mM EDTA, pH 4.6; also inhibits the phenoloxidase cascade) and bled. *In vivo* fungal cells were separated from insect haemocytes by 25–50 % step Centricoll gradient centrifugation as a pellet at the bottom of the centrifuge tube. Pellets were washed free of gradient material into the desired uptake buffer and used immediately. Collection of haemolymph, centrifugation and subsequent washing steps were all performed at 4 °C.

Lectins and chemical reagents. Fluorescently labelled lectins were obtained as follows. The Alexa Fluor 488-labelled lectins concanavalin A (ConA), *Griffonia simplicifolia* (GSII), *Helix pomatia* (HPA), *Griffonia simplicifolia* isolectin (GSI), peanut agglutinin (PNA) and wheatgerm agglutinin (WGA) were purchased from Molecular Probes-Invitrogen; the fluorescein-labelled lectins *Galanthus nivalis* (GNL), *Sambucus nigra* (SNA) and *Sophora japonica* (SJA), as well as the rhodamine-labelled lectins *Ricinus communis* I (RCA) and *Ulex europaeus* agglutinin I (UEAI), were purchased from Vector Laboratories; and the fluorescein-labelled *Limax flavus* (LFA) lectin was purchased from EY laboratories. Competing carbohydrates and

other chemicals and reagents were obtained from either Sigma-Aldrich or Fisher Scientific.

Treatment of cells with fluorescent lectins. Fungal cells were harvested by centrifugation (6000 ***g***, 5 min, 4 °C) and resuspended in the appropriate lectin binding buffer as listed in Table 1. Cells were treated with the lectin for 0.5–1.0 h, after which unbound lectin was removed by washing (three times) with the resuspension buffer before microscopic examination. At least 100 individual cells were examined for each sample, and all experiments were performed with at least three independently derived cell cultures.

Inhibitor treatments. Carbohydrate inhibition/completion experiments were performed by including specific inhibitory haptens during the initial reaction, as follows: ConA, 200 mM α-methyl mannoside and 200 mM α-methyl glucoside; GNL, 200 mM α-methyl mannoside; GSII, 500 mM α-*N*-acetylglucosamine; HPA, 500 mM α-*N*-acetylgalactosamine; GSI, 100 mM raffinose; PNA, 100 mM raffinose; UEAI, 100 mM fucose; WGA, 500 mM α-*N*-acetylglucosamine; RCA, 200 mM galactose; SNA, 200 mM lactose; LFA, 100 mM neuraminic acid; and SJA, 200 mM *N*-acetylgalactosamine.

Fluorescence microscopy and flow cytometry. Mounted slides were observed using a PASCAL LSM5 confocal microscope fitted with Nomarski differential interference contrast (DIC) optics. Observations were made on the single-celled propagules and on the tip and penultimate cells of growing hyphae, with basal cells also examined. Viability of the single-celled propagules was confirmed by propidium iodide (PI) staining and by taking aliquots and determining the percentage germination after overnight incubation in medium. Viability of hyphae was also confirmed by PI staining as well as by general appearance, presence of cytoplasmic streaming and observation of continued tip elongation and growth. Images were recorded with a real-time digital-imaging set-up and were arranged by Adobe Photoshop or similar software.

Fluorescent signals were quantified using a Becton Dickinson FACSort (fluorescence-activated cell sorter) using an argon laser, excitation wavelength 488 nm, emitted light detector 530 nm (±15 nm), adjusted to a fixed channel using standard Brite Beads (Coulter) prior to determining fluorescence. Samples were briefly vortexed before introduction to sheath fluid. Data acquisition and manipulation were performed with CellQuest and FACS Express v3, and fluorescence was measured for 20 000 conidia and submerged conidia, and 40 000 cells for all the other cell types assayed. Experiments were performed on at least two independent batches of cells.

High-pressure freezing, freeze-substitution and electron microscopy. Fungal cells were prepared for transmission electron microscopy (TEM) as follows. Samples were concentrated by centrifugation (12 000 r.p.m., 30 s) and the cell pastes transferred to type B planchettes (Technotrade). Samples were frozen using an HPM100 cell freezer (Leica) and freeze-substituted in dehydrated acetone containing 2 % OsO_4 at −80 °C for 2 days. The cell specimens were slowly warmed up to room temperature (1 °C h^{-1}) and washed thoroughly three times with acetone to remove OsO_4. After embedding in Embed 812 resin (Electron Microscopy Sciences) and polymerization, the cell specimens were sliced into 80 nm thin sections for TEM imaging. The 80 nm sections were post-stained with uranyl acetate solution (2 %, w/v) and subsequently with lead citrate solution (26 g lead nitrate $l^{-1}$and 35 g sodium citrate l^{-1}). Electron micrographs were captured with a Hitachi H-7000 transmission electron microscope operated at 80 kV. Freeze-substitution and slow warm-up were carried out using the AFS2 automatic freeze-substitution system (Leica).

RESULTS

Lectin binding profiles of *B. bassiana* aerial conidia, submerged conidia and *in vitro* blastospores

A series of 12 lectins with specificity to a range of carbohydrates was used to map the surface carbohydrate epitopes of *B. bassiana* aerial conidia, submerged conidia and three populations of *in vitro*-generated blastospores (see Table 1 for list of lectins used, their substrate specificities and the assay conditions). The different blastospore populations were derived from cells grown in rich broth medium (Sabouraud dextrose containing 0.5 % yeast extract) and protease peptone medium containing either lactose or trehalose. Aerial conidia and rich broth blastospores are the typical cell types used in biological control studies and applications. Trehalose is the major carbohydrate substituent of insect haemolymph, and lactose-grown cells were used for comparative purposes. A summary of the results of microscopic observations is presented in Fig. 1 and Table 2. In order to control for non-specific binding of the lectins, for all experiments, a sample reaction containing the inhibitory hapten, as listed in Table 1, was performed. Greater than 90 % inhibition of the lectin binding was observed in the presence of the competing sugar, except as noted below.

DIC images of the cell types coupled with visualization of the fluorescent lectin was used to assess the binding of the lectins to fungal cell surfaces (Fig. 1, Table 2). ConA, with specificity for α-glucose and α-*N*-acetylglucosamine (GlcNAc), bound to aerial conidia and somewhat patchily to submerged conidia, but did not bind to rich broth-, lactose- or trehalose-derived blastospores. GNL, which recognizes mannose residues, showed strong reactivity against submerged conidia and trehalose-derived cells, and weak reactivity to aerial conidia, *in vitro* blastospores and lactose-derived cells. GSII, specific for α- and β-GlcNAc, bound aerial conidia and submerged conidia, but did not bind to rich broth (*in vitro*) blastospores or lactose- and trehalose-derived cells. The HPA lectin, with specificity for α-*N*-acetylgalactosamine (GalNAc), was bound by aerial conidia, whereas GSI, recognizing α-galactose/α-GalNAc, reactivity was similar to that of ConA, binding aerial conidia and submerged conidia, but not reacting against any of the blastospore cell types. PNA and RCA, both of which recognize β-galactose, bound all cell types tested, although PNA bound only weakly to lactose-derived cells and RCA bound weakly to aerial conidia. SNA, which reacts with β-galactose and sialic acids only weakly, bound aerial conidia and submerged conidia, and did not bind any of the blastospore cell types. UEAI, which recognizes α-fucose, bound only aerial conidia. WGA, which recognizes β-GlcNAc and sialic acid residues, appeared to uniformly bind aerial conidia, with polarized spots clearly evident on submerged conidia and at the tips of the blastospore cell types. The lectins LFA and SJA, with specificity for sialic acid and β-GalNAc residues, respectively, displayed weak

Table 1. Lectins and assay conditions used in the study

Lectin	Abbreviation	Conjugate (Ex/Em) (nm)	Specificity	Inhibitor used	Storage buffer	Reaction buffer	Reaction concn
Concanavalin A	ConA	Alexa Fluor 488 (495/519)	α-Mannopyranosyl and α-glucopyranosyl residues	200 mM α-methyl mannoside and 200 mM α-methyl glucoside	0.1 M $NaHCO_3$, pH 8.3	PBS, 1.0 mM $CaCl_2$, 2.0 mM $MnCl_2$	60 μg ml^{-1}
Galanthus nivalis lectin	GNL	Fluorescein (494/518)	(α-1,3)Mannose	200 mM α-methyl mannoside	10 mM HEPES, 0.15 M NaCl, pH 7.5, 0.08 % sodium azide, 0.1 mM Ca^{2+}	10 mM HEPES, 0.15 M NaCl, pH 7.5	20 μg ml^{-1}
Griffonia simplicifolia lectin II	GSII	Alexa Fluor 488 (495/519)	α- or β-linked *N*-Acetyl-D-glucosamine	500 mM α-*N*-acetylglucosamine	PBS	PBS, 1.0 mM $CaCl_2$	20 μg ml^{-1}
Helix pomatia agglutinin	HPA	Alexa Fluor 488 (495/519)	α-*N*-Acetylgalactosamine residues	500 mM α-*N*-acetylgalactosamine	PBS	PBS, 1.0 mM $CaCl_2$	20 μg ml^{-1}
Griffonia simplicifolia isolectin	GSI	Alexa Fluor 488 (495/519)	*N*-Acetylgalactosamine or α-D-galactosyl residues	100 mM raffinose	PBS	PBS, 1.0 mM $CaCl_2$	20 μg ml^{-1}
Limax flavus agglutinin	LFA	Fluorescein (494/518)	Neuraminic acid and sialic acid	100 mM neuraminic acid	PBS	PBS, 1.0 mM $CaCl_2$	20 μg ml^{-1}
Peanut agglutinin	PNA	Alexa Fluor 488 (495/519)	Terminal β-galactose	100 mM raffinose	Sterile distilled water	PBS, 1.0 mM $CaCl_2$	20 μg ml^{-1}
Ricinus communis agglutinin I	RCA	Rhodamine (550/575)	Galactose or *N*-acetylgalactosamine	200 mM galactose	10 mM HEPES, 0.15 M NaCl, pH 7.5, 0.08 % sodium azide	10 mM HEPES, 0.15 M NaCl, pH 7.5	20 μg ml^{-1}
Sophora japonica agglutinin	SJA	Fluorescein (494/518)	β-*N*-Acetylgalactosamine	200 mM *N*-acetylgalactosamine	10 mM HEPES, 0.15 M NaCl, pH 7.5, 0.08 % sodium azide	10 mM HEPES, 0.15 M NaCl, pH 7.5	20 μg ml^{-1}
Sambucus nigra bark lectin	SNA	Fluorescein (494/518)	Sialic acid attached to terminal galactose in (α-2,6)	200 mM lactose	10 mM HEPES, 0.15 M NaCl, pH 7.5, 0.08 % sodium azide, 0.1 mM Ca^{2+}	10 mM HEPES, 0.15 M NaCl, pH 7.5	20 μg ml^{-1}
Ulex europaeus agglutinin I	UEAI	Rhodamine (550/575)	α-Linked fucose	100 mM fucose	10 mM HEPES, 0.15 M NaCl, pH 7.5, 0.08 % sodium azide	10 mM HEPES, 0.15 M NaCl, pH 7.5	20 μg ml^{-1}
Wheatgerm agglutinin	WGA	Alexa Fluor 488 (495/519)	*N*-Acetylglucosamine and *N*-acetylneuraminic acid residues	500 mM α-*N*-acetylglucosamine	0.1 M $NaHCO_3$, pH 8.3	PBS, 1.0 mM $CaCl_2$	20 μg ml^{-1}

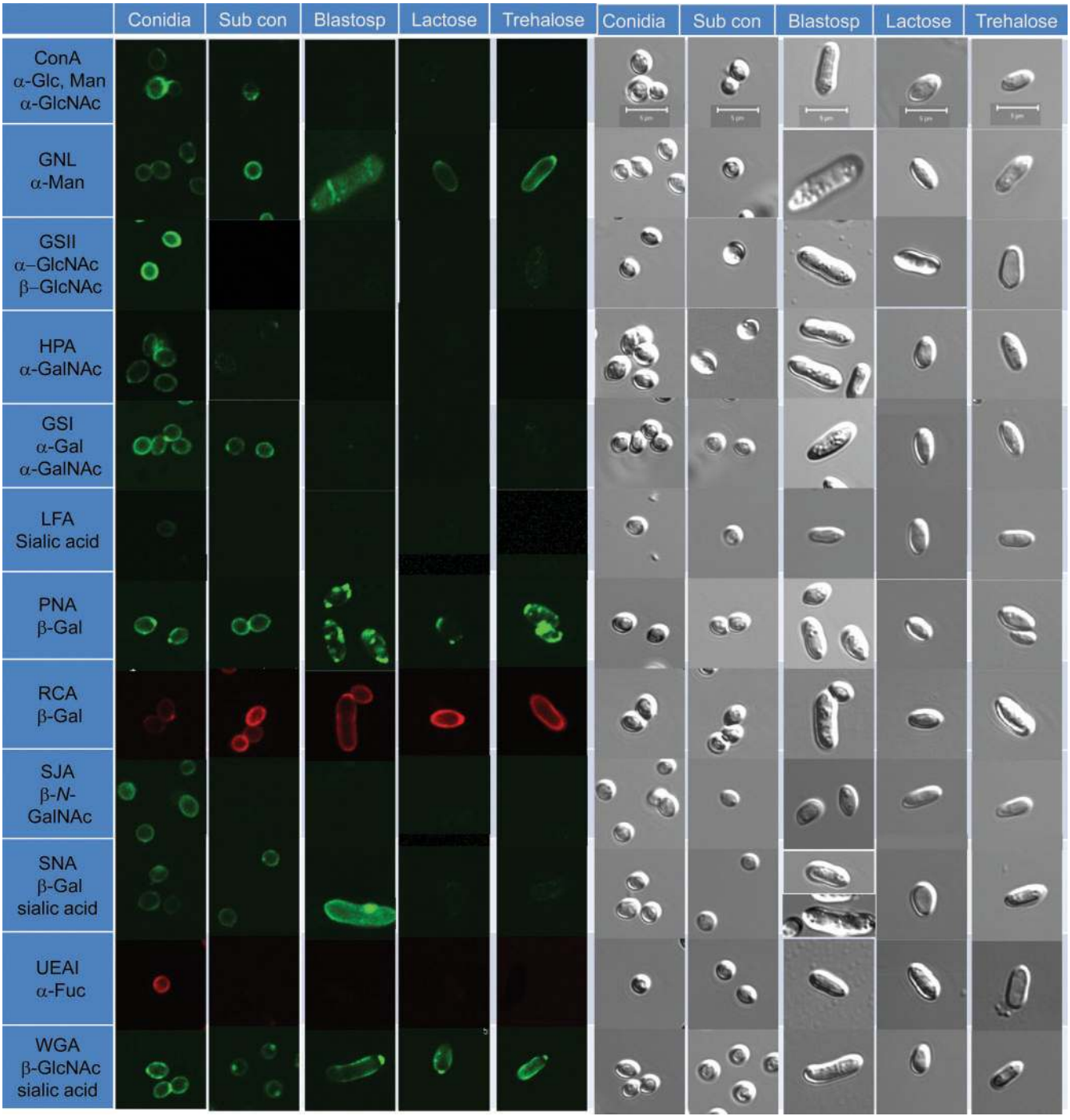

Fig. 1. DIC and fluorescence images of lectin binding profiles of *B. bassiana* aerial conidia, submerged conidia, *in vitro* blastospores, bile salts lactose- and bile salts trehalose-derived cells. Bars, 5 μm.

and inconsistent reactivity to aerial conidia and did not bind any of the other cell types tested.

Fluorescent lectin binding to the *B. bassiana* cell types was examined by flow cytometry, with representative profiles shown in Fig. 2 and a summary of the data presented in Table 2. These data allowed for an examination of the homogeneity of the response, as seen by the presence of shoulders and/or multiple peaks. Two populations of aerial conidia were apparent with respect to GNL and GSII, which contained distinct shoulders on the longer tail of the distribution (Fig. 2b), which represented ~10–20 % of the total counts. The SJA signal for aerial conidia contained two close but distinct peaks within the distribution (Fig.

Table 2. Summary of lectin binding to *B. bassiana* cell surfaces: flow cytometry and fluorescence microscopy

Lectin	Conidia	Submerged conidia	*In vitro* blastospores	Lactose-grown	Trehalose-grown	Hyphal bodies
ConA	15.1*	7.1	5.9, 1208	1.0	1.1	−§
	+†	+/−	−	+/−	+/−	
GNL	58.3‡, 94.8	142.0	450.0	81.0	358.7	126.2
	+	++	++	+	++	
GSII	84.3, 110	1.2	1.72	1.0	1.0	1.5
	++	−	−	−	−	
HPA	43.7	7.6	15.4, 110, 1922	1.0	1.0	−§
	+	++	++	−	−	
GSI	36.2	89.0	6.2, 1843.4	5.3	1.0	−§
	+	+	++	−	−	
LFA	10.9	7.2, 32	6.6, 453	1.0	1.7, 30	7.9
	+/−	−	+	−	−	
PNA	129.8	171.4	24.8, 120, 1100	62.0	27.1, 673.2	48.0
	++	+	++	++	++	
RCA§	+	++	++	++	++	++
SJA	17.3, 79.7	9.1, 45	5.8, 1252	1.0	1.5	1.6
	+	+	++	−	−	
SNA	56.0	54.9	30.8, 1928	1.1, 121	50.9	−§
	+	+	++	−	+/−	
UEAI§	++	−	−	−	−	−
WGA	124.7	37.2	245.8, 1050	80.7	57.3	240.9
	+	+	++	++	+	

*Mean log fluorescence calculated from flow cytometry data.
†Assessment of lectin binding as determined by the intensity of the detected fluorescence; ++, very bright fluorescent signal; +, readily detectable signal; +/−, weak signal; −, no signal detected.
‡Major peak underlined; more than one value underlined indicates multiple significant peaks.
§No flow cytometry data available.

2c). Similarly, the LFA and SJA distribution on submerged conidia showed two distinct peaks, although in contrast to the aerial conidia results, the peaks were much broader (Fig. 2d). *In vitro* blastospores appeared to contain the most heterogeneous subpopulations of lectin reactivity. Strong binding of the ConA, LFA, SJA, HPA, GSI and PNA lectins to small subpopulations of *in vitro* blastospores was evident, representing 1–5 % of the total cell population for the first three lectins and 5–10 % for the last three (LFA curve given in Fig. 2e). These observations were confirmed microscopically by the visualization of strong lectin binding to ~1–5 % of the cells examined (the images in Fig. 1 represent the typically observed response). Two significant peaks were noted for SNA binding to *in vitro* blastospores (Fig. 2f), which matched the microscopic visualization of these cells (see appropriate panel in Fig. 1). In addition, WGA, which resulted in a strong signal for most cells, contained a subpopulation with even greater apparent avidity. Lactose-grown cells showed low mean fluorescence values for ConA, GSII, HPA, GSI, LFA, SJA and SNA. Single, broad peaks were seen for GNL, PNA and WGA. Trehalose-grown cells gave similar results to those of lactose, with a few notable exceptions. Unlike for lactose-grown cells, the peaks obtained for trehalose-derived cells were sharper, indicating more homogeneous populations, and the mean log fluorescence for reactive lectins was notably higher. In addition, a clear signal could be detected with SNA, and a small subpopulation of cells (~1 %) appeared to display a low LFA signal. Trehalose-grown cells also showed two peaks with respect to PNA binding, with a small subpopulation (<5 %) displaying lower lectin binding. The flow cytometry data should be interpreted with some caution, since a large variation was noted for some fluorescent lectins between different cell preparations of the same cell type.

Lectin mapping reveals alterations in surface carbohydrates of germinated conidia

Germinated conidia displayed significant changes in lectin binding as compared with ungerminated conidia (Fig. 3). ConA binding to the conidia was retained, although a small polarized spot, localized to the emergence of the germ tube from the conidial base, could be seen for most germlings. Neither the germ tube itself nor the growing tip was stained with ConA. In contrast, GNL bound the conidial base as well as the entire length of the germ tube including the tip, whereas GSII bound the conidial base, up to the point at which the germ tube emerged, and did not bind any subsequent parts of the germ tube. HPA and GSI binding

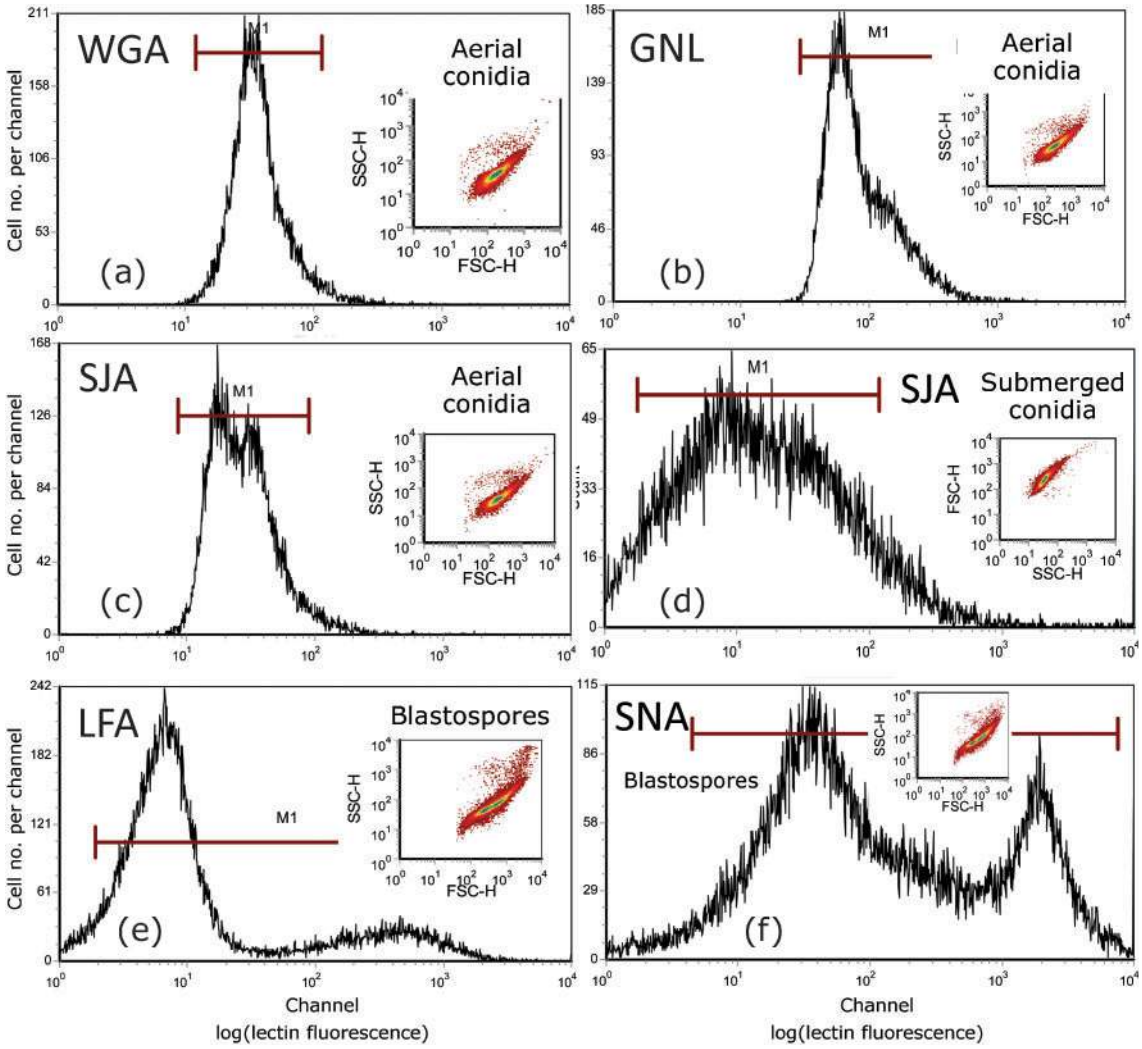

Fig. 2. Representative flow cytometry distributions of lectin binding by *B. bassiana* cells, illustrating the various responses observed. The lectin and cell type assayed are given in each panel. Distributions observed included: WGA + aerial conidia, sharp peak; GNL + aerial conidia, sharp peak with a distinct shoulder region; SJA + aerial conidia, two close, overlapping peaks; SJA + submerged conidia, broad peak; LFA + *in vitro*-derived blastospores, distinct low-fluorescent-intensity peak followed by small high-fluorescent-intensity peak; and SNA + *in vitro*-derived blastospores, two distinct peaks. Insets, side scatter versus forward scatter plots of the cell profiles passing through the detector.

was almost completely lost on germlings as compared with ungerminated conidia. Strong PNA and RCA binding was visible on germlings, although PNA binding at the conidial base was apparently lower than along the germ tube itself. Very faint SNA and SJA binding could be detected on the germlings, and complete loss of any LFA (very weak on aerial conidia to begin with) and UEAI (strong on ungerminated conidia) binding was seen. Although not consistent, in several instances complete inhibition of ConA and WGA binding to the conidia, and GNL binding to the germinated conidia, by the competing hapten was not observed, although the signal was greatly reduced. Furthermore, some variation in the intensity and distribution of several lectins, particularly ConA, GSII and PNA, on the various cell types was noted (as listed in Table 3, where the percentage of cells with the given response is listed).

In vivo haemolymph-derived *B. bassiana* cells

During infection of the insect host, the growing hyphae penetrate the cuticle, reaching the haemolymph, at which time the hyphae evolve single-celled yeast-like hyphal bodies that freely circulate within the insect haemolymph. This process was mimicked by direct intrahaemocoel injection of aerial conidia into host insects, resulting in the formation of *in vivo* haemolymph-derived cells within 2–4 days of injection. The *in vivo*-generated hyphal bodies

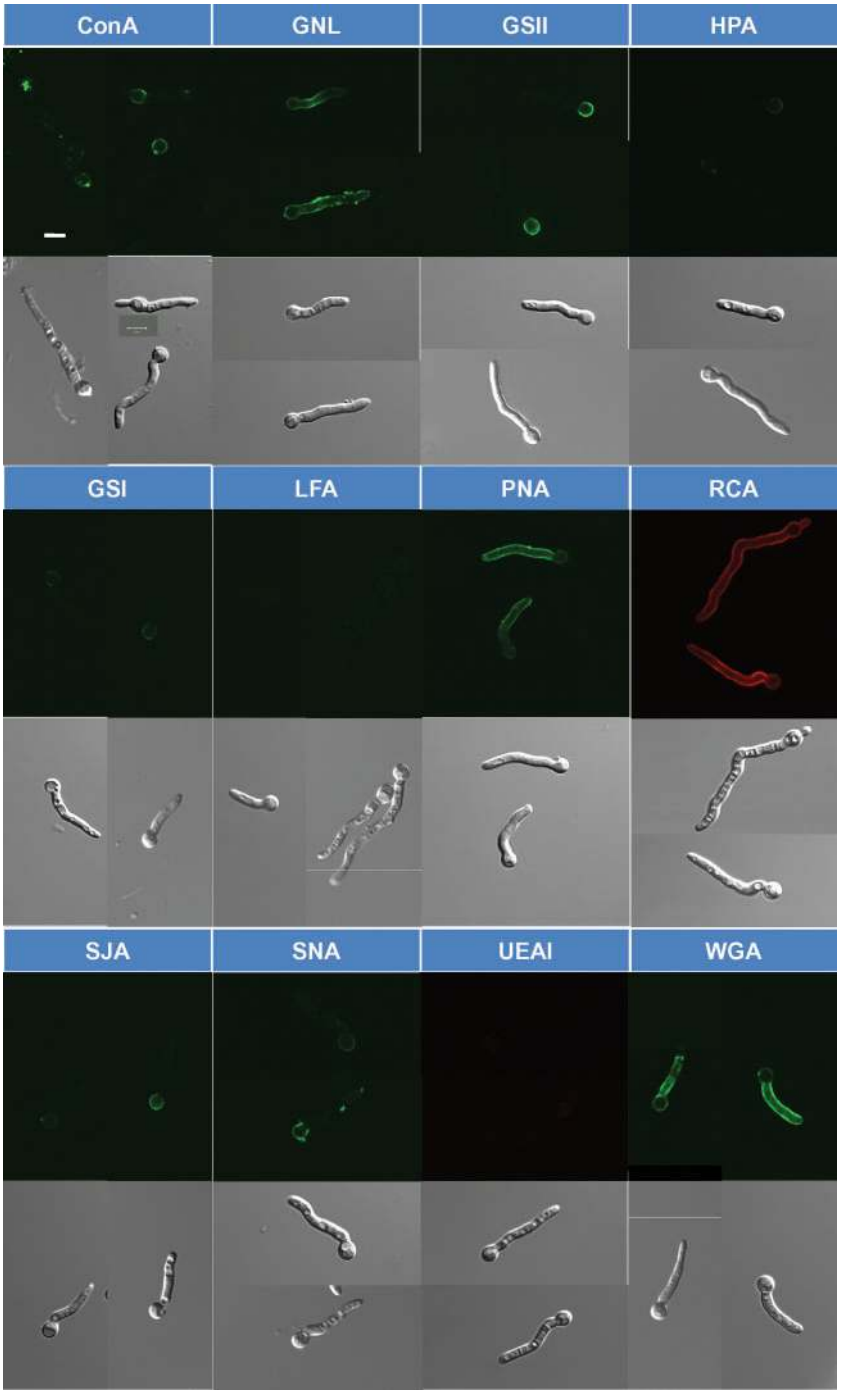

Fig. 3. DIC and fluorescence images of lectin binding profiles of *B. bassiana* germinated conidia. Bar, 5 μm.

were then isolated and separated from haemocytes and other haemolymph components by density-gradient centrifugation, as described in Methods. Very weak to no binding of the ConA, GSII, HPA, GSI, RCA, SNA, LFA and SJA lectins to *in vivo* hyphal bodies isolated from *Manduca sexta* was observed (Fig. 4, time zero). Occasional binding of the UEAI lectin was detected, although the signal was weak and not uniform. In contrast, GNL, PNA and WGA bound the haemolymph-derived fungal cells. Similar results were obtained using hyphal bodies isolated from *H. virescens*. In some instances, weak LFA, GSI, GSII and SJA binding was noted for *Manduca sexta* (and to a lesser extent for *H. virescens*) derived cells, although the signal was detected only on a subset of cells and variation was noted between experimental samples. Flow cytometry measurements of lectin binding to the haemolymph-derived hyphal bodies confirmed GNL and WGA binding, although both gave relatively broad peaks, implying heterogeneity in the response. Both PNA and LFA gave distinct peaks, although the mean log fluorescence values

Table 3. Summary of lectin binding to *B. bassiana* germinated conidia cell surfaces

Lectin	Germling		
	Conidial base	Hyphal walls	Hyphal apex
ConA	++* (>90 %)†	−	−
GNL	++ (>90 %)	++ (80 %)	++ (>90 %)
GSII	++ (>90 %)	−	−
HPA	+/− (>90 %)	−	−
GSI	+/− (>90 %)	−	−
LFA	−	−	−
PNA	+/− (>90 %)	++ (>90 %)	++ (>90 %)
RCA	++ (>90 %)	++ (>90 %)	++ (>90 %)
SJA	++ (50 %)	−	−
SNA	+/− (60 %)	−	−
UEAI	−	−	−
WGA	++ (>90 %)	++ (>90 %)	++ (>90 %)

*Assessment of lectin binding as determined by the intensity of the detected fluorescence; ++, very bright fluorescent signal; +, readily detectable signal; +/−, weak signal; −, no signal detected.
†Percentage of cells displaying the indicated signal.

were low. Incubation of the hyphal bodies in SAB over an 8 h time-course resulted in increased GNL, and more notably PNA and RCA, binding. Some SNA and SJA lectin reactivity was also noted, although the response was not consistent. Similar patterns of lectin reactivity were observed in cells that were placed into PBS or that were fixed in 2 % paraformaldehyde at each stage, although fixation of the cells typically resulted in reduced lectin binding and poorer quality images (data not shown).

Ultrastructural examination of the fungal cells

In order to determine whether any ultrastructural differences could be noted between the *in vitro*- and *in vivo*-derived fungal cells, particularly at the cell envelope, samples were prepared and examined by TEM by high-pressure freezing, as described in Methods. All of the *in vitro* cells examined, including aerial conidia, blastospores and lactose/trehalose-derived cells, contained a clearly visible opaque white zone that constituted the cell envelope (Fig. 5). Lipid bodies or storage vacuoles were clearly visible in aerial conidia that were rarely seen in the other cell types. Lactose-grown and rich broth (SAB)-grown *in vitro* blastospores gave essentially similar results (Fig. 5b). Trehalose-grown cells were similar to the other blastospore cell types, with the notable difference of containing large, often multiple, vacuoles not seen in the lactose or rich broth blastospores (Fig. 5c). In contrast to the *in vitro* cells, *in vivo* hyphal bodies derived from the haemolymph of *Manduca sexta* did not contain an opaque border region, and instead a highly ordered cell wall-bound brush-like structure appeared to completely surround the cells (Fig. 5d–f). Individual and distinct stems, topped with dense, bushy material, overall resembling palm trees, could be seen protruding from and contiguous with the cell wall. Similar results were obtained with fungal cells derived from *H. virescens* haemolymph.

DISCUSSION

Modulation of cell surface carbohydrates can affect a wide range of cellular processes, including adhesion, stress survival, and in the case of pathogens, immune invasion. Our data show that the carbohydrates that decorate the cell surface of the entomopathogenic fungus *B. bassiana* are stage and developmentally specific. Based upon the binding specificities of the lectins used coupled to the flow cytometry data, our data indicate that the surface carbohydrate epitopes of aerial conidia are the most diverse, and include glucose, galactose, mannose, GlcNAc, GalNAc and fucose. It is unclear whether they contain sialic acids, since although WGA, which also recognizes β-GlcNAc, binding was observed, only weak SNA (also binds to β-galactose), and very weak to no LFA (specific to sialic acids) binding was seen. Most of the carbohydrate epitopes found on the aerial conidia were not expressed on the germ tubes of germinated conidia. Thus, in contrast to ungerminated conidia, few to no glucose, α- or β-GalNAc, α-GlcNAc or fucose epitopes were detected along the germ tube of growing hyphae. Mannose and galactose continued to be found along the length of the germ tube including the tips of growing hyphae, although ConA, which recognizes mannose, α-glucose and α-GlcNAc, binding was not observed. This variation could be due to the fact that ConA has a combining oligosaccharide recognition that includes branched mannoses, whereas GNL recognizes Man(α-1,3)Man. WGA, indicating the presence of β-GlcNAc or sialic acids, was also observed to bind along the germ tube, although intriguingly, the tips of the growing hyphae did not appear to be labelled with the lectin in contrast to the binding of GNL, PNA and RCA. This was not due to plane-of-focus issues, which could obscure binding in some cases, since care was taken to observe specimens along a 3D axis. WGA binding does not appear to be due to the presence of sialic acids, since neither SNA nor LFA binding was observed; however, GSII binding, the specificity of which overlaps with that of WGA and includes α- and β-GlcNAc, was also not observed. Similar to ConA, the discrepancy between the WGA and GSII results is likely due to the influence of the combining sugar in their carbohydrate binding specificities. WGA recognizes GlcNAc(β-1,4)GlcNAc structures, whereas it is unclear what are the exact requirements for GSII binding.

Our data also revealed that the carbohydrates that decorate the conidia themselves (the conidial bases of germlings) change during the process of germination. Glucose, mannose, β-galactose and GlcNAc residues are retained on the conidial base after germination; however, α-GalNAc, α-galactose and fucose epitopes are lost. Thus, not only do the growing hyphae contain different surface carbohydrates

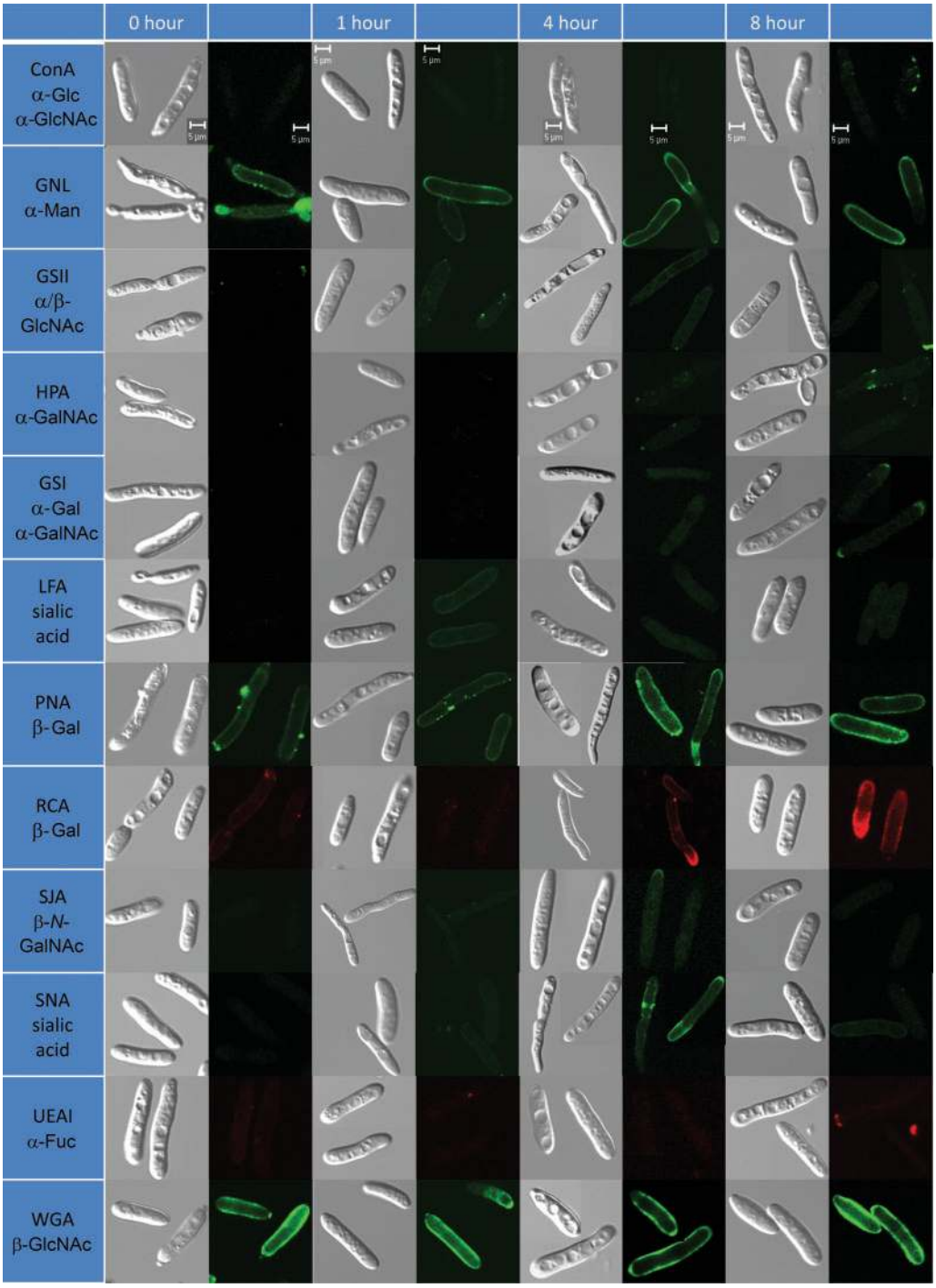

Fig. 4. DIC and fluorescence images of lectin binding profiles of *B. bassiana* hyphal bodies isolated from the haemolymph of *Manduca sexta*. Cells were either assayed immediately (time zero) or placed into SAB for the indicated time before addition of lectin, as described in Methods. Bars, 5 μm.

as compared with the conidia, but the conidia themselves undergo changes in surface sugar epitopes during germination and hyphal growth. The differences in lectin binding between resting spores and germlings, as well as variation along the germ tube, have been observed for the sclerotial mycoparasite *Coniothyrium minitans*, in which spore walls of germlings bind more ConA than the growing hyphae, hyphal walls bind more WGA, and hyphal apices bind more SBA than other regions of the germlings (Smith *et al.*, 1999). For *B. bassiana*, no ConA binding to the

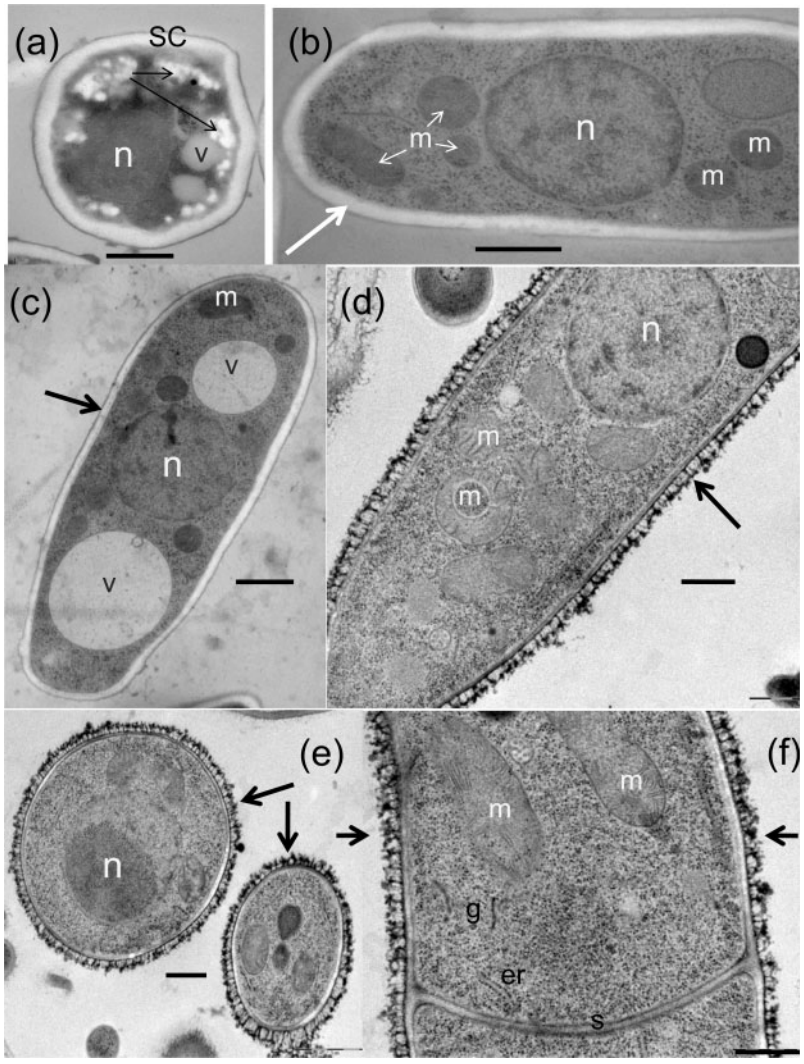

Fig. 5. TEM images of high-pressure frozen, freeze-substituted *B. bassiana* cells. Aerial conidia (a), lactose grown blastospores (b), trehalose grown blastospores (c) and *Manduca sexta* haemolymph-derived hyphal bodies (d–f). Cell walls/envelopes are marked by arrows; SC, spore coat; n, nucleus; m, mitochondrion; v, vacuole; LB, lipid body; g, golgi; er, endoplasmic reticulum; s, septum. Bars, 0.5 μm.

germlings was seen (only to the conidial base), and GNL, PNA, RCA and WGA binding could be seen along the germ tube to the tip, except in the case of WGA, which did not appear to label the apex of the growing germ tube.

In vitro blastospores and submerged conidia represent morphologically and biochemically distinct *B. bassiana* cells, considered to be adaptive responses to the availability of nutrients and nutrient deprivation, respectively (Bidochka *et al.*, 1987; Cho *et al.*, 2006; Thomas *et al.*, 1987). The surface carbohydrate epitopes of submerged conidia were very similar to those of aerial conidia, with the notable exception of the loss of fucose and β-GalNAc residues. Interestingly, WGA binding to submerged conidia appeared reduced in comparison with aerial conidia, with a clearly visible high-density lectin binding spot marking the cells. This may represent a bud scar or the labelling of a polar end of the cells for germination. *In vitro* blastospores appeared to retain only galactose and β-GlcNAc epitopes on their surfaces, with little to no glucose, mannose, GalNAc, fucose or sialic acids on their surfaces, although a small subset of cells appeared to retain carbohydrates, and indeed displayed greatly enhanced lectin binding, as evidenced by the flow cytometry data, which revealed ConA, HPA, GSI, LFA, PNA and SJA binding to 1–5 % of the cells examined. It is unclear whether this represents a small subset of cells that express multiple carbohydrates or individual subpopulations. Furthermore, PI staining of the cell types typically revealed 1–2 % morbidity of the cells, and it cannot be ruled out that some of the reactivity observed may have been due to non-specific adsorption of lectins by moribund cells. The binding of PNA to blastospore surfaces was distinctly non-uniform, with bright patches visible, and although RCA binding was uniform, this likely reflects variations in the densities of specific galactose epitope classes across the surface of blastospores, since the combining sugars for PNA and RCA are galactose(β-1,3)GalNAc and lactose, respectively. *In vitro* blastospores retained binding of WGA, and similar to the submerged conidia, a bright dense patch could be observed on most cells at one polar end of the cells. Since WGA binds to chitin oligosaccharides, this could represent the site of active chitin synthesis.

The rich diversity of surface carbohydrates found on aerial conidia is likely to contribute to the adhesion profiles observed with these cells, which bind hydrophobic surfaces well, but which can also adhere to hydrophilic surfaces, albeit weakly (Holder & Keyhani, 2005). However, it is unclear whether the carbohydrates detected would contribute to the net negative surface charge of aerial conidia at neutral pH (Holder *et al.*, 2007), particularly since little to no sialic acid, which would contribute to the surface charge, was detected. Studies on the adhesion of submerged conidia and blastospores have revealed that the former cells are able to bind a diverse range of substrata, including hydrophobic, weakly polar and hydrophilic surfaces, whereas the latter cells display some binding to weakly polar substrata but strong binding to hydrophilic surfaces (Holder & Keyhani, 2005). The relationship between the loss of fucose residues and the observed surface properties of submerged conidia is difficult to evaluate; however, the loss of multiple carbohydrate epitopes that might mask charged residues on the surface of *in vitro* blastospores as compared with aerial conidia is consistent with the idea that electrostatic charge plays a significant role in adhesion of these cells (Holder *et al.*, 2007).

When grown on bile salts/lactose media, *B. bassiana* produces yeast-like cells that retain their infectivity (Alves *et al.*, 2002). In addition to these lactose-grown cells, we also examined *B. bassiana* cells grown on similar media, with trehalose substituted for lactose, since trehalose is one of the major free carbohydrates found in insect haemolymph. Our data indicate that the surface carbohydrate epitopes of these cells are distinct from one another as well as different from aerial conidia and submerged conidia. Overall, trehalose-grown cells were similar to *in vitro* blastospores, except that they appeared to contain mannose epitopes which the blastospores did not contain. Similarly, lactose-grown cells contained mannose epitopes, but in addition contained α- and/or β-GlcNAc epitopes that did not appear to be uniformly distributed across the surface of the cells. Furthermore, PNA binding was also somewhat reduced and non-uniform; however, distinct WGA-labelled polar patches, which could represent sites of chitin synthesis, could be detected on both lactose- and trehalose-grown cells, similar to the results seen with *in vitro* blastospores and submerged conidia.

Surface mannose residues are known to modulate infection processes in pathogenic fungi, particularly in mammalian systems, where mannose binding protein is an important aspect of immune recognition of foreign cells. For *C. albicans*, the concentration of surface mannose residues as visualized by ConA binding has been found to be high in blastoconidia, low in the mother cell at germination, and high on the emerging germ tube (Tronchin *et al.*, 1989). Further measurements of *C. albicans* lectin avidity by flow cytometry have revealed the likelihood that lectins predominantly bind to a single receptor class and that use of multiple lectins with the same terminal carbohydrate specificity (e.g. to mannose) can yield important insights into the nature and abundance of these structures (Smith *et al.*, 2001). *In vivo*-produced *B. bassiana* cells circulate freely in the insect haemolymph and therefore appear to evade recognition by host immune cells. These hyphal bodies are osmotically sensitive, and previously it has been reported that these cells lose the mannose, GlcNAc and galactose on their surfaces, as evidenced by lack of ConA, WGA and *Spodoptera exigua* lectin (the last with presumed binding specificity for galactose residues) binding, respectively (Pendland *et al.*, 1993). Similarly, our data show that hyphal bodies derived from either *H. virescens* or *Manduca sexta* lose ConA binding. However, although this may reflect loss of some mannose epitopes, the hyphal bodies isolated from both insect hosts retained some mannose residues on their membranes, as determined by binding of GNL to these cells.

The presence of galactose residues (PNA binding) on the *in vivo*-derived hyphal bodies was observed, although RCA binding was lost, which likely reflects loss of certain galactose-terminated epitopes. Furthermore, a time-course of the hyphal bodies placed in rich broth medium revealed that the RCA-recognized epitope was one of the major attributes restored during the presumed dedifferentiation of these cells outside the host. It is also interesting to note that the *in vivo* cells differed from trehalose-grown cells by their (initial) lack of reactivity towards RCA. The haemolymph-derived hyphal bodies further appeared to contain β-GlcNAc as well as faint and non-uniform traces of fucose. Weak LFA binding was noted for aerial conidia, and only a minor signal was seen in insect-derived hyphal bodies, indicating the lack of appreciable amounts of surface sialic acids. This is in contrast to the role of these carbohydrates in the virulence of several fungi, notably the human pathogen *A. fumigatus*, in which increased surface sialic acid density on aerial conidia correlates with virulence (Wasylnka *et al.*, 2001). Overall, our data indicate the shedding of most carbohydrate epitopes by the *in vivo*-derived hyphal bodies. Since the lectins tested would react against epitopes that are linked to a variety of different molecules, including proteins, lipids and carbohydrate structures, loss of the binding of specific lectins, e.g. ConA and RCA, by the hyphal bodies likely reflects loss of specific classes of terminal carbohydrate-containing compounds and not complete loss of those carbohydrates from the cell surface.

Ultrastructural examination of the *B. bassiana* cell types revealed a unique brush-like outermost structure that has not, to our knowledge, been previously reported, although an electron-dense material was observed in a earlier study (Pendland *et al.*, 1993), which may represent a collapsed version of the structure observed in this study. Whereas a clear, opaque, cell envelope region was seen on all *in vitro* cell types examined, the cell walls of the haemolymph-derived hyphal bodies contained palm tree-like protrusions from their surfaces. Although this is speculative, this structure may mask the hyphal bodies from the host immune system, allowing for the free circulation of these cells. Surface fibrillar structures, either proteinaceous or carbohydrate in nature, some of which are thought to contribute to virulence and immune evasion, have long been noted on yeasts and

other fungi (Hazen & Hazen, 1993; Latgé *et al.*, 1988; Latgé, 2007; Osumi, 1998; Takeo *et al.*, 1993; Teertstra *et al.*, 2009). Further characterization of the composition and potential role of the *B. bassiana* material is warranted. The constant changes in the composition and presentation of surface carbohydrates on *B. bassiana* are likely to be relevant to host–insect interactions and imply the existence of stage-specific regulation of the molecules that bear these sugars and/or of glycosyltransferases and glycosidases that would mediate the observed variation in carbohydrate epitopes.

ACKNOWLEDGEMENTS

The authors wish to thank Neal Benson for assistance with the flow cytometry and Dr B. H. Kang for his assistance with the electron microscopy.

REFERENCES

Alves, S. B., Rossi, L. S., Lopes, R. B., Tamai, M. A. & Pereira, R. M. (2002). *Beauveria bassiana* yeast phase on agar medium and its pathogenicity against *Diatraea saccharalis* (Lepidoptera: Crambidae) and *Tetranychus urticae* (Acari: Tetranychidae). *J Invertebr Pathol* **81**, 70–77.

Bidochka, M. J., Pfeifer, T. A. & Khachatourians, G. G. (1987). Development of the entomopathogenic fungus *Beauveria bassiana* in liquid cultures. *Mycopathologia* **99**, 77–83.

Cho, E. M., Liu, L., Farmerie, W. & Keyhani, N. O. (2006). EST analysis of cDNA libraries from the entomopathogenic fungus *Beauveria* (*Cordyceps*) *bassiana*. I. Evidence for stage-specific gene expression in aerial conidia, *in vitro* blastospores and submerged conidia. *Microbiology* **152**, 2843–2854.

Esquenazi, D., de Souza, W., Alviano, C. S. & Rozental, S. (2003). The role of surface carbohydrates on the interaction of microconidia of *Trichophyton mentagrophytes* with epithelial cells. *FEMS Immunol Med Microbiol* **35**, 113–123.

Hazen, K. C. & Hazen, B. W. (1993). Surface hydrophobic and hydrophilic protein alterations in *Candida albicans*. *FEMS Microbiol Lett* **107**, 83–88.

Holder, D. J. & Keyhani, N. O. (2005). Adhesion of the entomopathogenic fungus *Beauveria* (*Cordyceps*) *bassiana* to substrata. *Appl Environ Microbiol* **71**, 5260–5266.

Holder, D. J., Kirkland, B. H., Lewis, M. W. & Keyhani, N. O. (2007). Surface characteristics of the entomopathogenic fungus *Beauveria* (*Cordyceps*) *bassiana*. *Microbiology* **153**, 3448–3457.

Latgé, J. P. (2007). The cell wall: a carbohydrate armour for the fungal cell. *Mol Microbiol* **66**, 279–290.

Latgé, J. P., Bouziane, H. & Diaquin, M. (1988). Ultrastructure and composition of the conidial wall of *Cladosporium cladosporioides*. *Can J Microbiol* **34**, 1325–1329.

Latgé, J. P., Kobayashi, H., Debeaupuis, J. P., Diaquin, M., Sarfati, J., Wieruszeski, J. M., Parra, E., Bouchara, J. P. & Fournet, B. (1994). Chemical and immunological characterization of the extracellular galactomannan of *Aspergillus fumigatus*. *Infect Immun* **62**, 5424–5433.

Lewis, M. W., Robalino, I. V. & Keyhani, N. O. (2009). Uptake of the fluorescent probe FM4-64 by hyphae and haemolymph-derived *in vivo* hyphal bodies of the entomopathogenic fungus *Beauveria bassiana*. *Microbiology* **155**, 3110–3120.

Lis, H. & Sharon, N. (1986). Lectins as molecules and as tools. *Annu Rev Biochem* **55**, 35–67.

Masuoka, J. (2004). Surface glycans of *Candida albicans* and other pathogenic fungi: physiological roles, clinical uses, and experimental challenges. *Clin Microbiol Rev* **17**, 281.

Osumi, M. (1998). The ultrastructure of yeast: cell wall structure and formation. *Micron* **29**, 207–233.

Pendland, J. C. & Boucias, D. G. (1984). Use of labeled lectins to investigate cell-wall surfaces of the entomogenous hyphomycete *Nomuraea rileyi*. *Mycopathologia* **87**, 141–148.

Pendland, J. C. & Boucias, D. G. (1986). Lectin binding characteristics of several entomogenous hyphomycetes – possible relationship to insect hemagglutinins. *Mycologia* **78**, 818–824.

Pendland, J. C. & Boucias, D. G. (1992). Ultrastructural-localization of carbohydrate in cell-walls of the entomogenous hyphomycete *Nomuraea rileyi*. *Can J Microbiol* **38**, 377–386.

Pendland, J. C. & Boucias, D. G. (1993). Variations in the ability of galactose and mannose-specific lectins to bind to cell-wall surfaces during growth of the insect pathogenic fungus *Paecilomyces farinosus*. *Eur J Cell Biol* **60**, 322–330.

Pendland, J. C. & Boucias, D. G. (1996). Phagocytosis of lectin-opsonized fungal cells and endocytosis of the ligand by insect *Spodoptera exigua* granular hemocytes: an ultrastructural and immunocytochemical study. *Cell Tissue Res* **285**, 57–67.

Pendland, J. C., Hung, S. Y. & Boucias, D. G. (1993). Evasion of host defense by *in vivo*-produced protoplast-like cells of the insect mycopathogen *Beauveria bassiana*. *J Bacteriol* **175**, 5962–5969.

Sharon, N. (2007). Lectins: carbohydrate-specific reagents and biological recognition molecules. *J Biol Chem* **282**, 2753–2764.

Sharon, N. & Lis, H. (1993). Carbohydrates in cell recognition. *Sci Am* **268**, 82–89.

Smith, S. N., Armstrong, R. A., Barker, M., Bird, R. A., Chohan, R., Hartell, N. A. & Whipps, J. M. (1999). Determination of *Coniothyrium minitans* conidial and germling lectin avidity by flow cytometry and digital microscopy. *Mycol Res* **103**, 1533–1539.

Smith, S. N., Armstrong, R. A., Bird, R. A., Chohan, R., Hartell, N. A. & Poyner, D. A. (2001). Characterization of FITC-conjugated lectin binding to *Candida albicans*. *Mycologia* **93**, 422–431.

Takeo, K., Mine, H., Nishimura, K. & Miyaji, M. (1993). The existence of a dispensable fibrillar layer on the wall surface of mycelial but not yeast cells of *Aureobasidium pullulans*. *FEMS Microbiol Lett* **111**, 153–158.

Tartar, A. & Boucias, D. G. (2004). A pilot-scale expressed sequence tag analysis of *Beauveria bassiana* gene expression reveals a tripeptidyl peptidase that is differentially expressed *in vivo*. *Mycopathologia* **158**, 201–209.

Teertstra, W. R., van der Velden, G. J., de Jong, J. F., Kruijtzer, J. A. W., Liskamp, R. M. J., Kroon-Batenburg, L. M. J., Muller, W. H., Gebbink, M. F. B. G. & Wösten, H. A. B. (2009). The filament-specific Rep1-1 repellent of the phytopathogen *Ustilago maydis* forms functional surface-active amyloid-like fibrils. *J Biol Chem* **284**, 9153–9159.

Thomas, K. C., Khachatourians, G. G. & Ingledew, W. M. (1987a). Production and properties of beauveria-bassiana conidia cultivated in submerged culture. *Can J Microbiol* **33**, 12–20.

Tronchin, G., Bouchara, J. P. & Robert, R. (1989). Dynamic changes of the cell-wall surface of *Candida albicans* associated with germination and adherence. *Eur J Cell Biol* **50**, 285–290.

Warwas, M. L., Watson, J. N., Bennet, A. J. & Moore, M. M. (2007). Structure and role of sialic acids on the surface of *Aspergillus fumigatus* conidiospores. *Glycobiology* **17**, 401–410.

Wasylnka, J. A., Simmer, M. I. & Moore, M. M. (2001). Differences in sialic acid density in pathogenic and non-pathogenic *Aspergillus* species. *Microbiology* **147**, 869–877.

Edited by: B. A. Horwitz